



# Removal and determination of Malachite Green dye using nanofiber membranes and UV-Vis spectrophotometer

Ahmed Jaber Ibrahim<sup>\*a</sup>, Juman A. Naser<sup>b</sup>, Emad. S. Taiyh<sup>a</sup>, Zahraa F. Hassan<sup>c</sup>, and Jeehan H. Mohammed<sup>a</sup>

<sup>a</sup>Scientific Research Center, Al-Ayen Iraqi University, ThiQar 64011, Iraq

<sup>b</sup>University of Baghdad, College of Education for Pure Science- Ibn Alhaitham, Department of Chemistry, Iraq

<sup>c</sup>College of Dentistry, Al-Ayen Iraqi University, Thi-Qar 64011, Iraq

## ARTICLE INFO:

Received 3 Feb 2025

Revised form 12 Apr 2025

Accepted 15 May 2025

Available online 30 Jun 2025

## Keywords:

Adsorption,  
Malachite Green,  
UV-Vis spectrophotometer,  
Nanofiber membranes,  
Electrospinning technique,  
Isotherms

## ABSTRACT

The removal of malachite green (MG) dye on nanofiber membranes, which were prepared by the electrospinning technique, was studied after preparing a suitable resin to act as an efficient adsorbent. A UV-Vis spectrophotometer determined the MG concentration. The morphology of nanofiber membranes with an average diameter of 550 nm was studied by SEM, EDX, and XPS techniques. The batch approach was used to study the factors affecting the adsorption, which included the effect of equilibrium time, the adsorbent dose, the initial dye concentration, and temperature. The adsorption isotherms were also studied according to the Freundlich and Langmuir models and the thermodynamic functions. The results showed that the maximum adsorption efficiency was 92.946% at 318 K, and the adsorption capacity of the adsorbent was 18.4 mg g<sup>-1</sup>. Analytical chemistry features such as the limit of detection (LOD: 0.3 mg L<sup>-1</sup>), limit of quantification (LOQ: 0.9 mg L<sup>-1</sup>), and linear range (1-50 mg L<sup>-1</sup>) were obtained. From the correlation coefficient values, it was found that the Langmuir model is more suitable than the Freundlich model for describing the general adsorption isotherm. Also, the amount of dye molecule adsorption increases with increasing temperature (Endothermic Process), and there is more random movement on the nanofiber membrane than in the aqueous solution. The process occurs spontaneously as indicated by the positive values of  $\Delta H^\circ$  and  $\Delta S^\circ$  and the negative value of  $\Delta G^\circ$ .

## 1. Introduction

The presence of synthetic dyes in wastewater, particularly from textile and industrial effluents, poses significant environmental and health challenges [1]. Among these dyes, Malachite Green (MG) is of particular concern due to its widespread use and potential toxicity. MG, a cationic dye, is extensively employed in various industries such as aquaculture, textile, and paper manufacturing.

However, its persistence in the environment and resistance to biodegradation necessitate the development of effective removal strategies [2]. Traditional methods for dye removal, including chemical oxidation, coagulation, and biological treatments, often suffer from limitations such as incomplete removal, high operational costs, and the generation of secondary pollutants [3]. In recent years, adsorption has emerged as a promising alternative due to its simplicity, efficiency, and cost-effectiveness. The key to successful adsorption lies in the selection of an appropriate adsorbent with a high surface area, specific affinity for the target

\*Corresponding Author: [Ahmed Jaber Ibrahim](mailto:Ahmed Jaber Ibrahim)

Email: [ahmed.jbrahim@alayen.edu.iq](mailto:ahmed.jbrahim@alayen.edu.iq)

<https://doi.org/10.24200/amecj.v8.i02.1012>

pollutant, and ease of regeneration [4,5]. Recent advancements in nanotechnology have opened new avenues for developing effective adsorbents capable of efficiently removing dyes from contaminated water [6]. Among these, nanofiber membranes produced by electrospinning have garnered considerable attention due to their unique properties, including high surface area, tunable porosity, and the ability to functionalize surfaces to enhance adsorption capacity [7]. Electrospinning, a versatile and scalable technique, allows for the precise fabrication of nanofiber membranes, offering an innovative approach to creating adsorbents with superior performance [8]. This study aims to explore the potential of nanofiber membranes prepared via electrospinning for the removal of Malachite Green dye from aqueous solutions. The research focuses on the comprehensive preparation and characterization of these membranes, followed by a detailed examination of their adsorption behavior through isotherm models. Furthermore, thermodynamic studies will be conducted to elucidate the nature of the adsorption process, providing insights into the spontaneity, feasibility, and effectiveness of using electrospun nanofiber membranes in dye removal applications. This investigation not only contributes to the understanding of the adsorption mechanisms involved but also highlights the potential of electrospun nanofiber membranes as a sustainable and efficient solution for wastewater treatment, particularly in removing hazardous dyes like Malachite Green. In previous studies, we discussed several different scientific aspects in various scientific fields, but we found this topic worth exploring due to its scientific importance [9-17].

## 2. Materials and methods

### 2.1. Instruments

Electrospinning Machine (Model-NE300, Inovenso Ltd. Co., Turkey), UV-Vis spectrophotometer (Model-1780, Shimadzu CO., Japan), Scanning electron microscope (SEM; Model-Inspect S50, FEI Co., USA), Energy-dispersive X-ray (EDX; Model-Quantax EDS for SEM Xflash 6/10, Bruker Co., German), X-ray Photoelectron Spectrometer (XPS; Model-K-Alpha, Thermo Fisher Scientific Inc., USA), Shaking Water Bath (Model-SWB-25, HYSC Ltd., South Korea), Electronic Analytical Balance (Hawach Sci., P.R.China), Oven electrically heated (Nabertherm GmbH., German), and Hotplate Magnetic Stirrer (Infitek Co., Ltd., P.R.China) were used in this study.

### 2.2. Materials and Reagents

Table 1 shows the chemicals and their specifications used in this study, as well as the distilled water used to prepare the solutions.

### 2.3. Preparation of nanofiber membranes

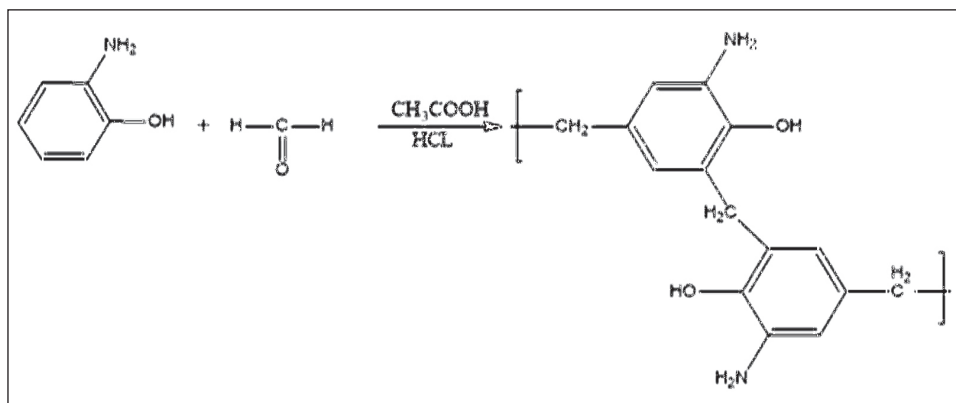
Nanofiber membranes are prepared by electrospinning of a resin prepared by reacting 8 g of 2-aminophenol with 2.5 ml of formaldehyde at 80°C, and the presence of acetic acid/concentrated hydrochloric acid in a ratio of (10:1) as a catalyst, as in the following reaction (Equation 1).

Then, a 30% (w/v) resin solution and a 20% (w/v) polystyrene solution were prepared using DMF as a solvent. The spinning solution was prepared from the prepared resin solution and polystyrene solution in a ratio of (1:9) after mixing them homogeneously

**Table 1.** Explains the chemicals used and some of their specifications

Materials	Formula	M.W (g mol <sup>-1</sup> )	Purity (%)	Source	CAS No
Glacial Acetic Acid	CH <sub>3</sub> CO <sub>2</sub> H	60.05	99	BDH	64-19-7
Formaldehyde	CH <sub>2</sub> O	30.03	37	Sigma	50-00-0
2-aminophenol	C <sub>6</sub> H <sub>7</sub> NO	109.13	99	Sigma	95-55-6
Hydrochloric acid	HCl	36.5	99	BDH	7647-01-0
DMF	C <sub>3</sub> H <sub>7</sub> NO	73.10	99	Sigma	68-12-2
Polystyrene (PS)	(C <sub>8</sub> H <sub>8</sub> ) <sub>n</sub>	(104) n	99	Sigma	9003-53-6
Malachite Green	C <sub>23</sub> H <sub>25</sub> N <sub>2</sub> Cl	364.92	99	BDH	569-64-2

**DMF:** N, N-Dimethylformamide



(Eq.1)

and then transferred to the electrospinning device and the spinning settings were adjusted, which include the mixing pump speed ( $0.03 \text{ ml min}^{-1}$ ), the rotating cylinder speed (50 rpm), the applied voltage (32 kV), and the distance between the pump and the spinning cylinder (15 cm) to obtain the nanofiber membranes and then placed in a drying oven at a temperature of  $50 \text{ }^\circ\text{C}$  to become ready for use as adsorbent surfaces.

#### 2.4. Preparation of standard solution

The standard Malachite Green (MG) dye used in this study was prepared at a concentration of  $500 \text{ mg L}^{-1}$  by dissolving 0.5 g of the dye in 1000 mL of distilled water. From this, different solutions were prepared at various concentrations. The maximum wavelength

( $\lambda_{\text{max}}$ ) of 616 nm was determined using a UV-Vis spectrophotometer with a wavelength range of 200–800 nm, as shown in Figure 1. The calibration curve, which illustrates the relationship between absorbance and concentration, was created using the following six concentrations: 5, 10, 15, 20, 40, and  $50 \text{ mg L}^{-1}$ , as shown in Figure 2, after measuring the absorbance of these concentrations at the dye's  $\lambda_{\text{max}}$ .

#### 2.5. Surface morphology study of prepared nanofiber membranes

The morphology of the prepared nanofiber surfaces was studied by scanning electron microscopy (SEM), energy dispersive X-ray spectroscopy (EDX), and X-ray photoelectron spectroscopy (XPS) to identify their chemical and physical

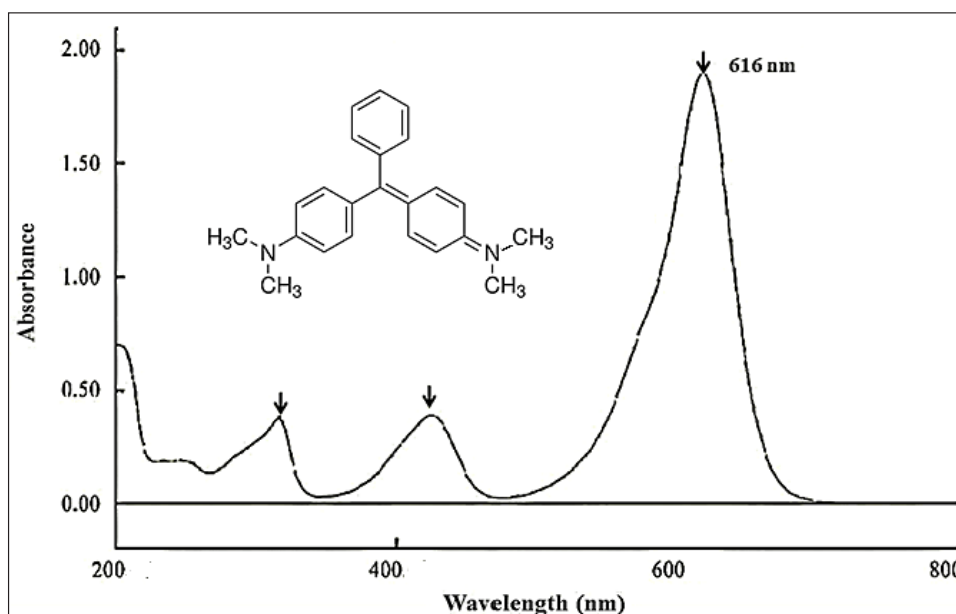
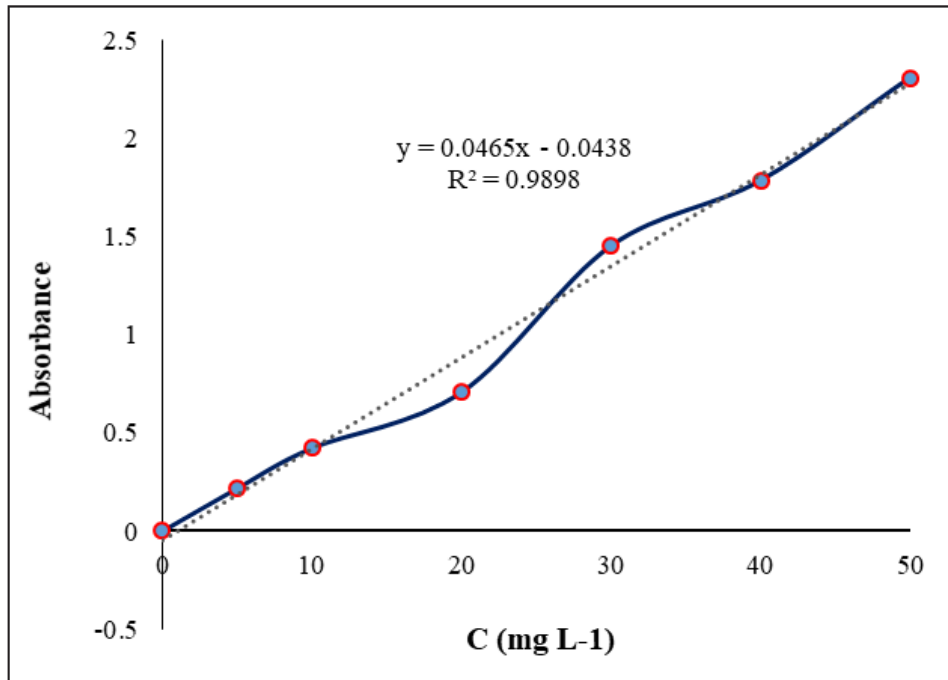


Fig. 1. UV-Vis spectrum of Malachite Green (MG) dye



**Fig. 2.** Calibration curve of Malachite Green (MG) dye.

properties and to determine their surface area. [Figure 3](#) shows the shape, size, and dimensions of the nanofibers obtained in the SEM analysis after coating the tested sample with a thin layer of gold and platinum, where a network of continuous and homogeneous nanofibers with an average nanofiber diameter of 550 nm is observed, and the swelling that occurs at low viscosity does not appear. The results of the homogeneity of the nanofibers and

the average thinness of the obtained nanofibers are attributed to the chemical and physical properties of the prepared resin, as well as the spinning conditions, which directly affect the shape, size, and diameter of the nanofibers. Generally, increasing the surface area ratio of the nanofiber membranes makes them a material with very effective adsorbent properties [7]. [Figure 4](#) shows the energy dispersive X-ray (EDX) analysis to determine the chemical properties of

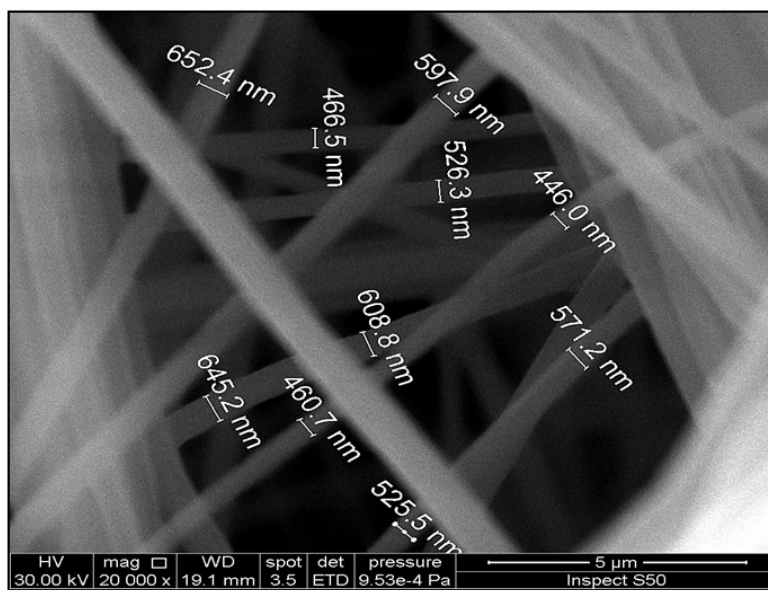


**Fig. 3.** Scanning Electron Microscopy (SEM) analysis of the prepared nanofiber membranes

the prepared nanofibers by knowing the atomic elements that make them up. The weight percent (%) of the elements was also obtained as in Table 2. The high weight percentage of carbon (88.04 %) in the nanofibers indicates the main components of the prepared resin, as in Equation 1, in addition to the presence of a weight percentage of nitrogen (2.55 %) attributed to the amine group. It is also noted that a small percentage of chlorine (0.53 %) is attributed to the hydrochloric acid residues used as a catalyst in the resin preparation. In contrast, the appearance of small percentages of gold and platinum (1.48% and 0.7 %, respectively) is attributed to the materials used to coat the samples in the SEM analysis. Also, the special percentage

of aluminum (6.1 %) is attributed to the aluminum foil used to cover the collecting cylinder of the nanofibers during the electrospinning process [8]. To study the chemical composition and oxidation states of the prepared nanofibers' surface more precisely, X-ray photoelectron spectroscopy (XPS) analysis was performed, as shown in Figure 5. Three prominent peaks appear in the XPS spectrum at the following binding energy values: C1s (at around 285 eV), N1s (at around 400 eV), and O1s (at around 530 eV). The C1s peak (around 285 eV) indicates the carbon atoms in the compound which typically correspond to C–C, C–H, and CH<sub>2</sub> bonds, which are present in polystyrene and the carbon chains of 2-aminophenol-formaldehyde (the

**Table 2.** Weight percentages of atomic elements in EDX analysis of the prepared nanofiber membranes

Element	Atomic number	Series	[wt.%]
Carbon	6	K-series	88.04232
Aluminum	13	K-series	6.100238
Nitrogen	7	K-series	2.553872
Gold	79	L-series	1.489128
Platinum	78	L-series	0.702431
Chlorine	17	K-series	0.532012
Sum	---	---	99.420011

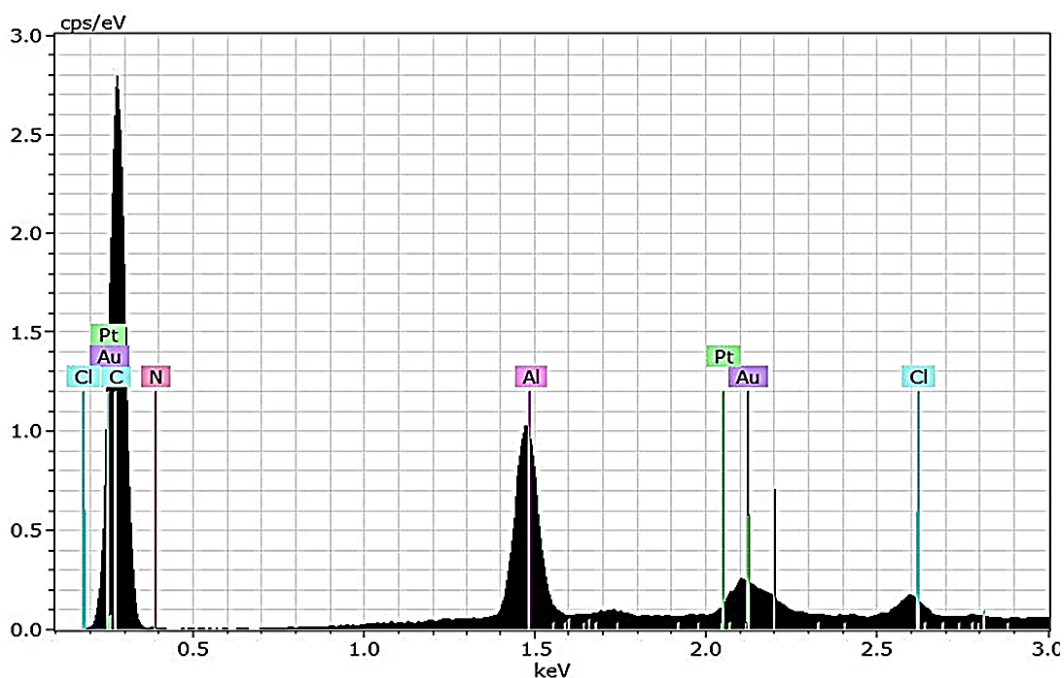


**Fig. 4.** Energy Dispersive X-Ray (EDX) analysis of the prepared nanofiber membranes

main components of the prepared nanofibers) and there may also be a contribution from the C=O bond present in phenol. Also, this C 1s peak indicates carbon in a low oxidation state, as expected in polystyrene. The N 1s peak (around 400 eV) shows the presence of nitrogen in the compound, which typically corresponds to N-H or N-C bonds, which would be expected in 2-aminophenol-formaldehyde. The lack of a significant shift in binding energy indicates that nitrogen is still in an oxidation state close to its natural oxidation state (-3), which corresponds to amine (NH<sub>2</sub>) or N-C bonds present in the nanofibers. The O 1s value (around 530 eV) indicates the presence of oxygen in the compound, which typically corresponds to C=O bonds (such as carbonyls) or O-C bonds (such as ethers) or the contribution of several oxygen species including O-H from the hydroxyl groups in 2-aminophenol, or oxygen in the ether bonds (C-O-C) present in the structure. The O 1s peak at 530 eV indicates that oxygen is present in several different oxidation states (presence of a mixture of C=O, C-OH, and O-C bonds). It suggests the diversity of the chemical composition of the nanofibers and their surface loading [18].

## 2.6. Adsorption process

The adsorption of Malachite Green (MG) dye onto the prepared nanofiber membranes was investigated using a batch approach under different conditions. A specific amount of adsorbate (prepared nanofiber membranes) was mixed with 20 ml of dye solution in 100 ml flasks using a shaking water bath to study all adsorption experiments. UV-Vis spectroscopy was used to monitor the dye concentration before and after the adsorption process at the maximum wavelength ( $\lambda_{max}$ ) of 616 nm. Equation 2 was used to calculate the amount of adsorbate material ( $Q_e$ ) in units of mg g<sup>-1</sup> [19].

$$Q_e = \frac{V_{sol} (C_o - C_e)}{m} \quad (\text{Eq.2})$$

$Q_e$ : amount of adsorbate in unit mg g<sup>-1</sup>;  $V_{sol}$ : total volume of adsorbate solution in unit L;  $C_o$ : initial concentration of adsorbate solution in unit mg L<sup>-1</sup>;  $C_e$ : concentration of adsorbate solution at equilibrium in unit mg L<sup>-1</sup>;  $m$ : weight of adsorbent material in units of g

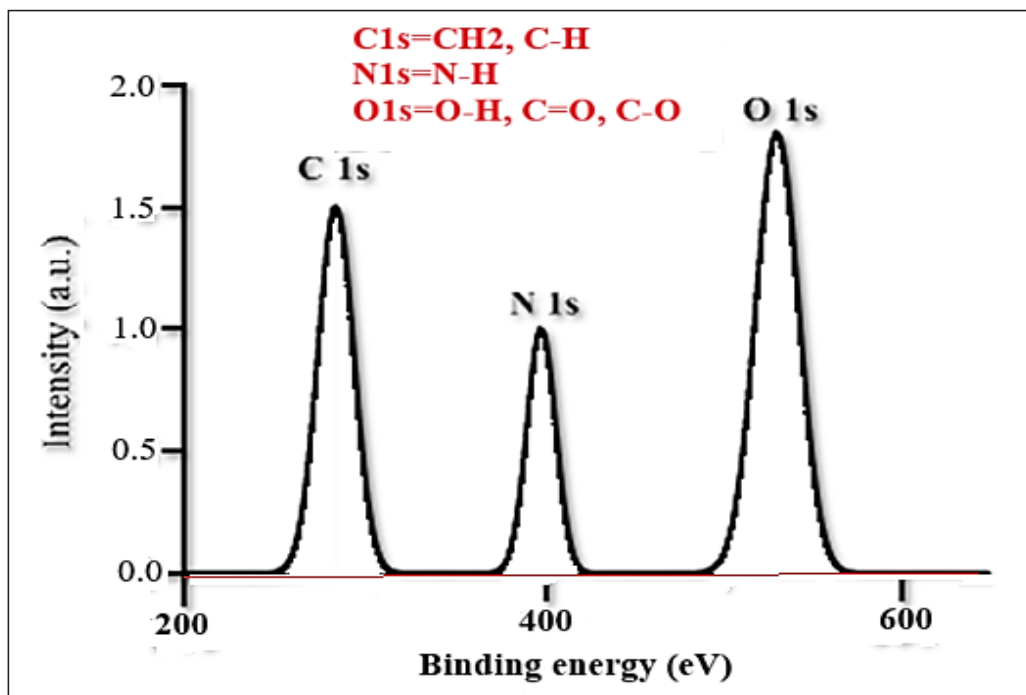


Fig. 5. X-ray photoelectron spectroscopy (XPS) analysis of the prepared nanofiber membranes

### 3. Results and Discussion

#### 3.1. Study the factors affecting the adsorption

##### 3.1.1. The effect of equilibrium time

To study the effect of equilibrium time required for the absorption of MG dye on the nanofiber prepared membranes, a solution of MG dye was prepared at a concentration of  $40 \text{ mg L}^{-1}$  and then placed in direct contact with  $0.004 \text{ g}$  of nanofiber prepared membranes in a  $100 \text{ ml}$  flask and put in a temperature-controlled shaking water bath (fixed shaking speed of  $120 \text{ rpm}$ ). The temperature was fixed at  $298\text{K}$ , and the flask was shaken continuously for different periods ( $15, 30, 45, 60, 120, 150, 180,$  and  $210 \text{ min}$ ) after which the concentration of MG dye was investigated at those periods using a UV-Vis spectrometer. The results showed that the best period for equilibrium to occur is  $150 \text{ min}$ , as shown in Figure 6. Nanofibers have a relatively large surface area compared to other materials and therefore provide more adsorption sites for the dye, which increases the adsorption rate as seen in Figure 6 [20]. However, once all adsorption sites on the surface are filled, the process starts to slow down until equilibrium is reached at about  $150 \text{ min}$ . In the beginning, adsorption is fast due to the high concentration of dye in the solution and many empty sites on the surface of the nanofibers.

However, as time passes, the diffusion process within the nanofibers and surface layers becomes slower, as the molecules are more confined in the multiple adsorption layers, which increases the time required to reach equilibrium [21].

##### 3.1.2. The effect of adsorbent dose

To study the effect of the adsorbent dose of the prepared nanofiber membranes for the adsorption process of Malachite Green (MG) dye, six different doses ( $0.001\text{-}0.006 \text{ g}$ ) were taken and placed in direct contact with the dye solution in 6 flasks, and the adsorption process was carried out under fixed experimental conditions (initial dye concentration  $40 \text{ mg L}^{-1}$ , equilibrium time  $150 \text{ min}$ , shaking speed  $120 \text{ rpm}$ , and  $298\text{K}$ ). The results showed that the best weight of the adsorbent dose was  $0.004 \text{ g}$ , as shown in Figure 7. It is observed at the beginning that the amount of adsorbate dye increases ( $Q_e$ ) with the increase in the dose of nanofibers due to the large surface area and efficient physical and chemical properties of the fibers, which leads to an increase in the adsorption efficiency. However, after a weight of  $0.004 \text{ g}$  or more, the adsorption capacity begins to slow down, indicating the saturation of the effective adsorption sites, such that no more effective sites are available on the nanofibers to adsorb the dye [22].

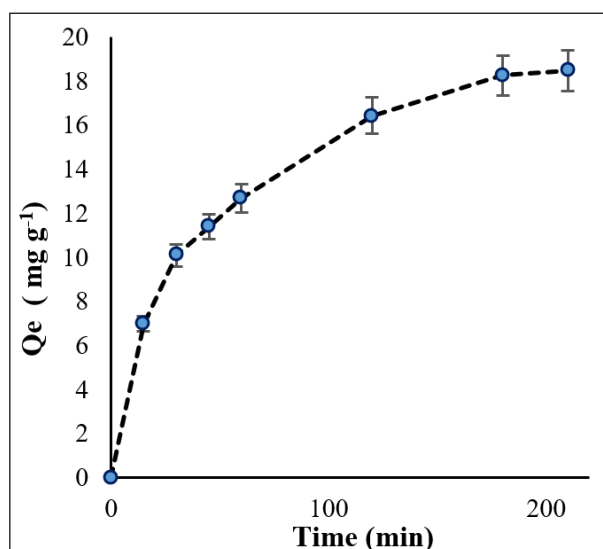


Fig. 6. The effect of equilibrium time

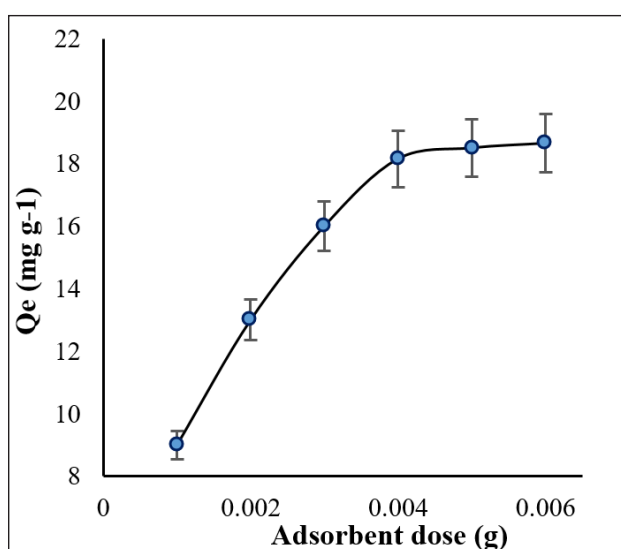


Fig. 7. The effect of adsorbent dose

### 3.1.3. The effect of initial dye concentration

To study the effect of initial dye concentration on the adsorption process, eight different initial dye concentrations (15-50 mg L<sup>-1</sup>) were taken and placed in direct contact with prepared nanofiber membranes in 8 flasks. The adsorption process was conducted under fixed experimental conditions (adsorbent dose 0.004 g, equilibrium time 150 min, shaking speed 120 rpm, and 298 °K). The results showed that the best initial dye concentration was 40 mg L<sup>-1</sup>, as shown in Figure 8. It is noted that the amount of adsorbate dye ( $Q_e$ ) increases with the increase of the initial dye concentration until it reaches a concentration of 40 mg L<sup>-1</sup> and begins to slow down and decrease at higher concentrations. This indicates that the active sites on the nanofibers are almost saturated with dye molecules. When the concentration increases more than that, competition occurs between the dye molecules or even an increase in their size, making them less effective in adsorption [23].

### 3.1.4. The effect of temperature

To study the effect of temperature on the adsorption process of Malachite Green (MG) dye on the prepared nanofiber membranes, the adsorption process was carried out at different temperatures

(298, 303, 308, 313, and 318°K) under constant experimental conditions (adsorbent dose 0.004 g, equilibrium time 150 min, shaking speed 120 rpm, and initial dye concentration 40 mg L<sup>-1</sup>). The results showed that the adsorption process increases with increasing temperature, as shown in Figure 9. It is noted that the amount of adsorbent dye ( $Q_e$ ) increases with increasing temperature on the prepared nanofibers, i.e. the adsorption process is Endothermic, and this can be explained by the fact that increasing temperature leads to the expansion of the surface, which leads to an increase in its porosity and surface area, which results in an increase in the penetration of dye molecules into the internal pores of the nanofiber surface on the one hand, and on the other hand, an increase in the contact of dye molecules with the internal active sites that are present within the composition of the prepared resin used in the spinning process to form the nanofiber. Also, increasing temperature works to strengthen the bonds between the adsorbate dye (MG) and the adsorbent surface higher than it is from the bonding force between the dye molecules (solute) and water (solvent), i.e. the adsorption forces overcome the solute-solvent interference forces. The dominance of these forces increased with increasing temperature [24].

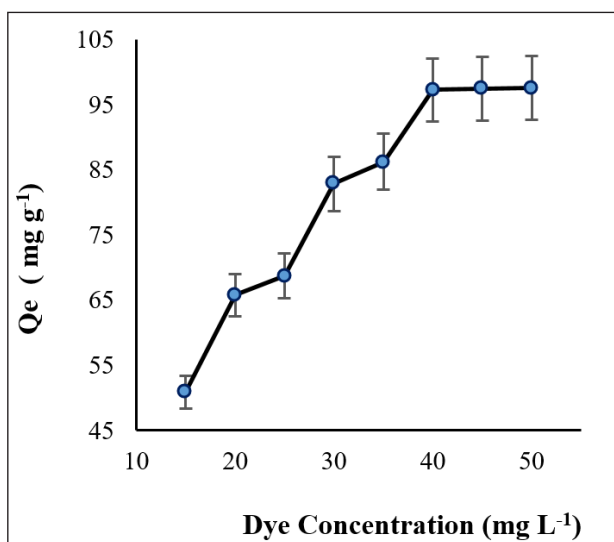


Fig. 8. The effect of initial dye concentration

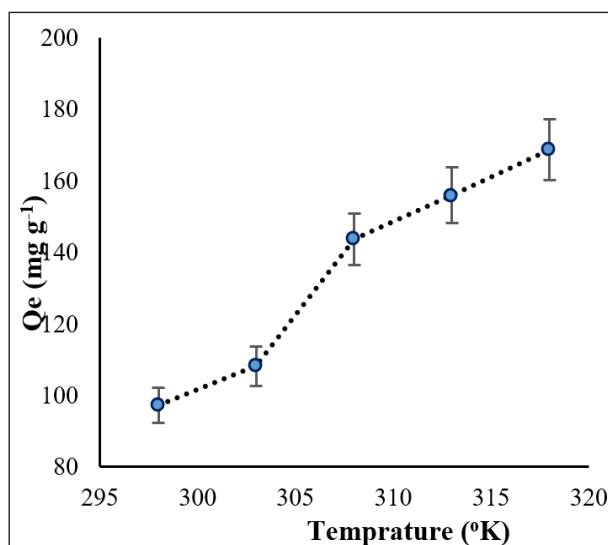


Fig. 9. The effect of temperature

### 3.2. Adsorption Percentage

Table 3 shows the percentage adsorption (%) of Malachite Green (MG) dye onto the prepared nanofiber membranes at different temperatures and under constant experimental conditions (adsorbent dose 0.004 g, equilibrium time 150 min, shaking speed 120 rpm, and initial dye concentration 40 mg L<sup>-1</sup>). Equation 3 was used to calculate the adsorption percentage [22]. It is noted from Table 3 above that the percentage of adsorption increases with increasing temperature. The adsorption rate at the last temperature (318 K) reached 92.94%. This means that the adsorption process has reached its maximum at that temperature and that a small amount of dye remains in the solution, which qualifies for using these membranes in practical aspects, the most important of which is water filtration systems [8].

$$\text{Adsorption (\%)} = \frac{(C_o - C_e)}{C_o} * 100$$

(Eq.3)

### 3.3. Adsorption Isotherms

#### 3.3.1. Freundlich model

The Freundlich equation was used to process the adsorption data of Malachite Green (MG) dye on the prepared nanofiber membranes within the temperature range of 298, 303, 308, 313, and 318 °K to investigate the adsorption isotherms [22].

$$\ln Q_e = \ln K_f + \frac{1}{n} \ln C_e$$

(Eq.4)

Q<sub>e</sub>: amount of adsorbate in unit mg g<sup>-1</sup>; C<sub>e</sub>: concentration of adsorbate solution at equilibrium in unit mg L<sup>-1</sup>; n and K<sub>f</sub>: Freundlich constants.

The Freundlich constants are obtained from the linear relationship of a special curve it consists of the x-axis representing the values of lnC<sub>e</sub> and the y-axis representing the values of lnQ<sub>e</sub> where the slope represents K<sub>f</sub> (which reflects a capability for surface adsorption) and the intercept represents n, as shown in Figure 10.

Table 4 notes that the values of the K<sub>f</sub> constant generally increase with increasing temperature, except for its value at 313 °K, which show a slight deviation from the general behavior. This means that the adsorption process increases with increasing temperature in general. The K<sub>f</sub> constant expresses the ability of the adsorbate to adsorb at a certain equilibrium. Usually, increasing the temperature leads to an increase in the kinetic energy of the molecules, which enhances the movement of the dye molecules and increases the possibility of their collision with the surface of the nanofibers, thus increasing the amount of adsorption. Therefore, a general increase in the K<sub>f</sub> value can be observed with increasing temperature [25].

Despite the general trend of increasing K<sub>f</sub> with temperature, the slight deviation at 313°K may be due to specific effects such as changes in the properties of the nanofiber surface at this temperature, or there may be a change in the interaction between the dye and the nanofibers as a result of slight changes in the surface structure or surface energy at this specific temperature [26]. As for the n constant, a relative decrease in its value is observed with increasing temperature,

**Table 3.** Absorption percentage of Malachite Green (MG) dye on prepared nanofiber membranes at different temperatures

Temperature (°k)	Adsorption Percentage (%)
298	9.075
303	13.591
308	16.387
313	85.795
318	92.946

except at 318 °K. The  $n$  constant expresses the adsorption strength, as high values indicate that the adsorption is stronger and tends towards multilayer adsorption. The decrease in  $n$  with increasing temperature means that the adsorption becomes less strong and may be less preferable to multilayer adsorption, perhaps as a result of the increase in the kinetic energy of the molecules that may weaken the bonding forces between the dye molecules and

the surface of the nanofiber membranes [25]. The exception in the value of  $n$  constant at 318 °K may be due to a change in the thermodynamic equilibrium of adsorption, which leads to a preference or change in the adsorption mechanism that becomes more coherent at this temperature. Other factors may intervene, such as rearrangement of the nanoscale surface or other effects at the molecular level that affect how the dye molecules interact with the

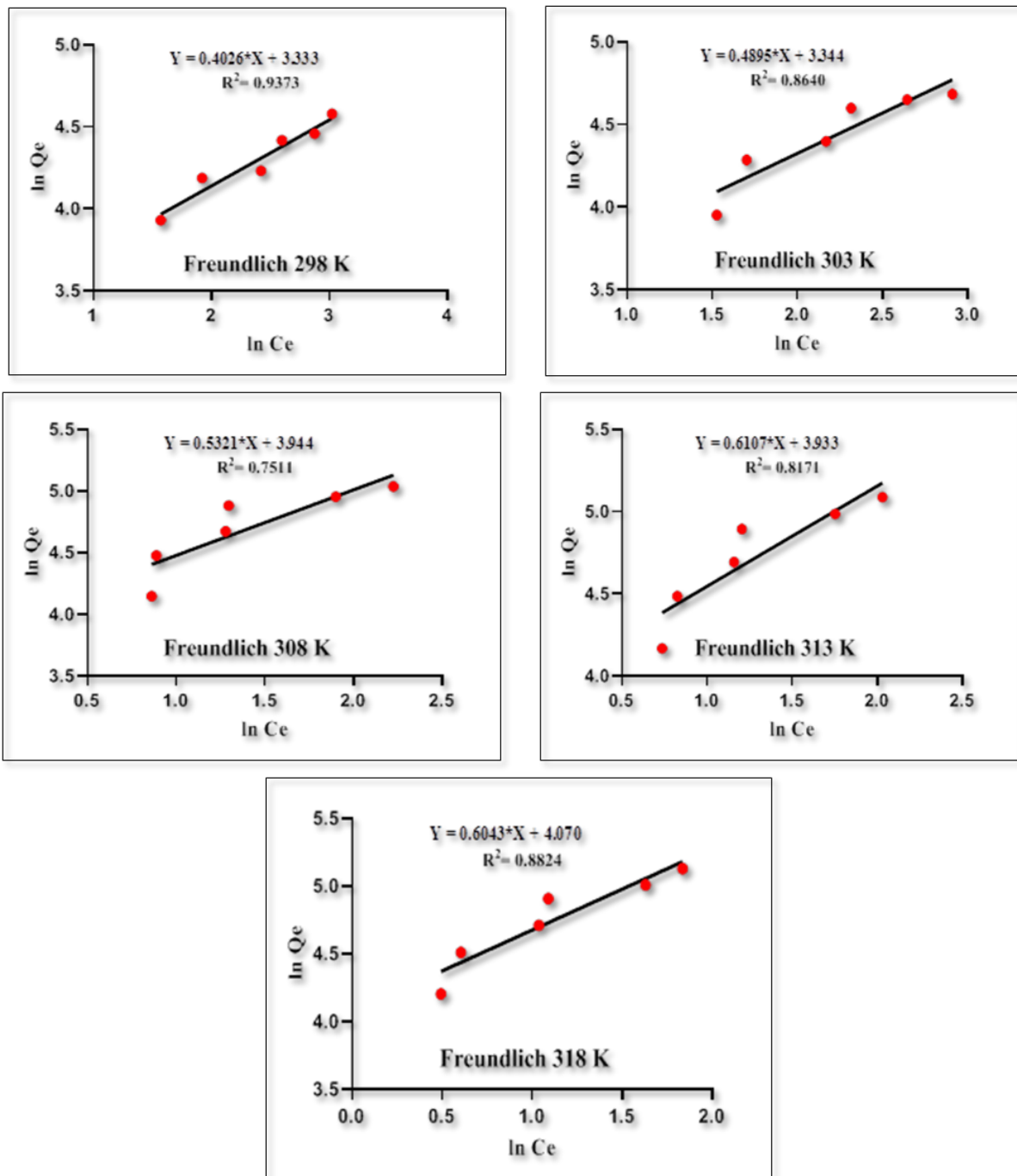


Fig. 10. Plots of  $\ln C_e$  vs  $\ln Q_e$  for adsorption of MG dye

**Table 4.** The Freundlich parameters for the MG dye adsorption on nanofiber membranes.

Temperature (K)	$k_f$ $k_f$ (mg L <sup>-1</sup> )	$n$	$R^2$
298	27.994	2.488	0.937
303	28.332	2.045	0.864
308	51.573	1.880	0.751
313	51.060	1.639	0.817
318	58.498	1.656	0.882

surface at this specific temperature [27]. On the other hand, when calculating the numerical average of the coefficient of determination ( $R^2$ ) values for all the studied temperatures, it was equal to 0.85. This value is generally considered good, but it is not ideal, which means there are some differences between the experimental results and the predictions provided by the Freundlich model. In general, these behaviors indicate that the adsorption process of MG dye on prepared nanofiber membranes is complex and is affected by several factors related to the interactions between the molecules (MG dye) and the surface of the adsorbent (prepared nanofiber membranes), which may vary based on subtle thermal changes [28].

### 3.3.2. Langmuir model

The Langmuir equation was used to process the adsorption data of Malachite Green (MG) dye on the prepared nanofiber membranes within the temperature range of 298, 303, 308, 313, and 318 °K to investigate the adsorption isotherms [29]. The Langmuir constants are obtained from the linear relationship of a special curve. It consists of the x-axis representing the values of  $C_e$  and the y-axis representing the values of  $C_e/Q_e$ , where the slope represents  $1/Q_{e\max}$  and the intercept represents  $1/Q_{e\max} K_1$ , as shown in Figure 11.

$$\frac{C_e}{Q_e} = 1/Q_{\max} \cdot k_1 + C_e/Q_{\max} \quad (\text{Eq.5})$$

$Q_e$ : amount of adsorbate in units mg g<sup>-1</sup>,  $C_e$ : concentration of adsorbate solution at equilibrium in units mg L<sup>-1</sup>,  $K_1$  and  $Q_{e\max}$ : Langmuir constants. Table 5 notes that the value of the KL constant

increases relative to temperature, except for its values at 313 °K and 318 °K, which showed a slight deviation from the general behavior. This means an increase in the dye adsorption equilibrium with increasing temperature on the adsorbent surface (prepared nanofiber membranes) and thus an increase in the adsorption capacity [30].

The  $K_1$  constant expresses the adsorption equilibrium and is related to the adsorption energy. Usually, with the increase in temperature, the energy of molecules increases, which leads to the increased mobility of dye molecules and the possibility of their collision with the surface of nanofibers, thus promoting the adsorption process. Therefore, it is natural that the value of  $K_1$  increases with the increase in temperature [31]. The slight deviation in the  $K_1$  value at 313 K and 318 K could be due to changes in the physical or chemical nature of the nanofiber surface at these temperatures. For example, a change in the structural composition of the nanofibers or the surface interactions may occur that may lead to changes in the ability of the surface to attract dye molecules, thus affecting the value of the  $K_1$  constant [26]. The same applies to the maximum adsorption capacity ( $Q_{e\max}$ ), which increases with increasing temperature, except for its value at 318 °K, which deviates from the general behavior. The  $Q_{e\max}$  constant expresses the maximum adsorption capacity (i.e., the maximum amount of dye that can be adsorbed on the surface of the nanofibers). Typically, as the temperature increases, the activity of the molecules and their ability to diffuse inside the pores of the adsorbent material (prepared nanofiber membranes) increases, which increases the maximum adsorption capacity ( $Q_{e\max}$ ) [32]. The anomaly at 318 °K may be due to changes in the surface structure of the nanofibers

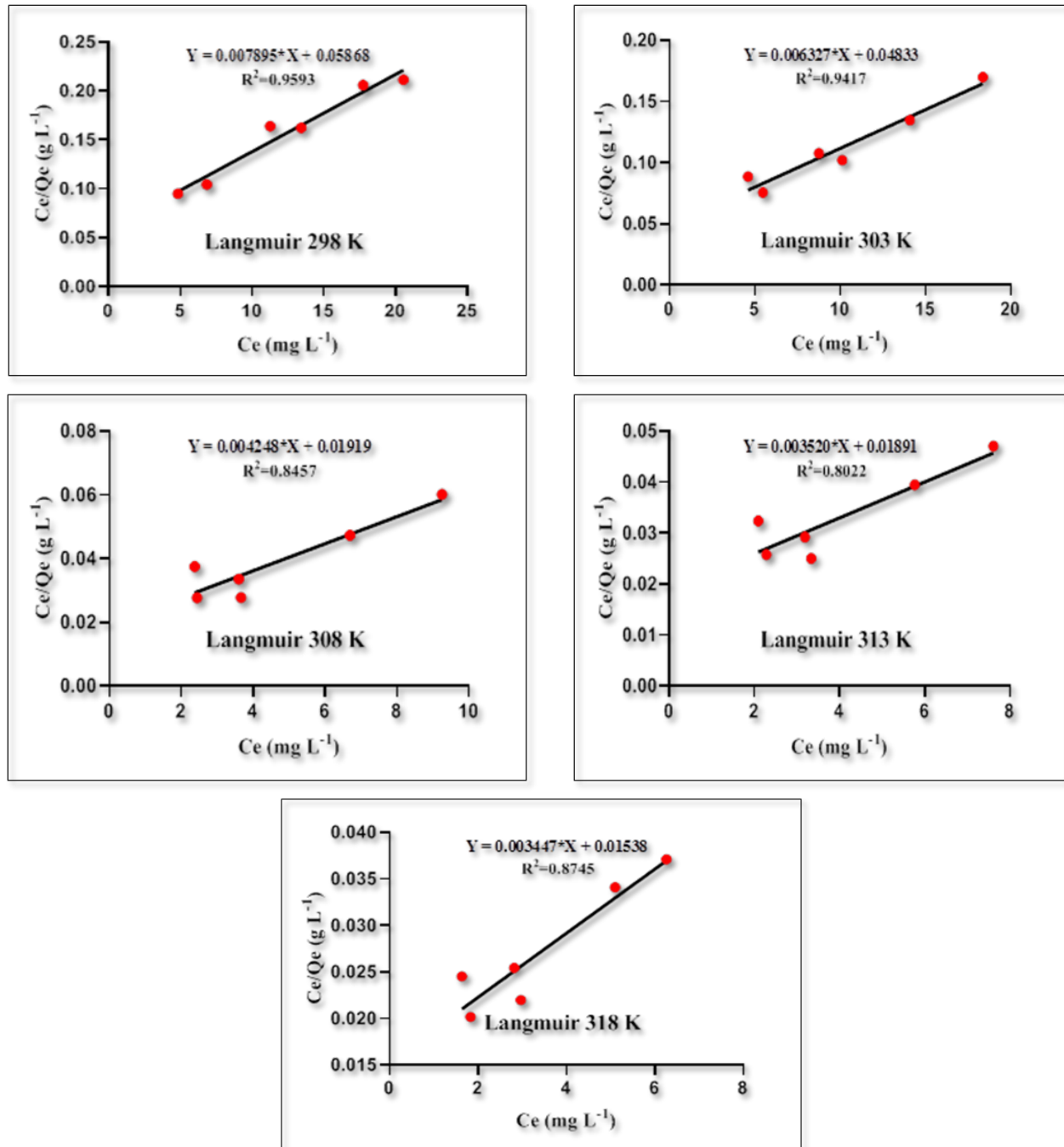


**Fig. 11.** Plots of  $C_e$  vs  $C_e/Q_e$  for adsorption of MG dye on prepared nanofiber membranes

**Table 5.** The analytical Langmuir parameters for the MG dye adsorption

Temperature (K)	$Q_e$ max ( $\text{mg L}^{-1}$ )	$K_1$ ( $\text{L mg}^{-1}$ )	$R^2$
298	142.857	0.120	0.959
303	166.666	0.125	0.941
308	250	0.210	0.845
313	333.333	0.166	0.802
318	333.333	0.2	0.874

or the interaction between the dye and the surface at this temperature. There may be a phase transition or rearrangement of the surface of the nanofibers at this temperature, which reduces the number of active sites available for adsorption or affects the interaction between the surface molecules and the dye molecules [33]. The observed behavior of the Langmuir isotherm can be explained by the thermodynamic and physical changes that affect the interactions between the dye molecules and the nanofiber surface with temperature. While the general trend is for the adsorption constants and maximum capacity to increase with temperature, deviations from this behavior can be due to surface- and interaction-specific effects at certain temperatures, such as 313 °K and 318 °K. Also, the numerical average of the coefficient of determination ( $R^2$ ) values of the Langmuir equation for all the studied temperatures reached 0.884, which means that the model provides a reasonably good explanation of the adsorption behavior of Malachite Green (MG) dye molecules on the prepared nanofiber membranes, but it is not entirely ideal. On the other hand, when comparing the average values of the coefficient of determination ( $R^2$ ) of the Langmuir equation (0.884) versus the Freundlich equation (0.85), we find that it is more applicable to the Langmuir equation. Thus, this model is more suitable for describing the adsorption isotherm. Many techniques, such as GC-MS and GC-FID, are also used to determine dyes and organic compounds in waters and other matrices [34-41].

### 3.4. Thermodynamics adsorption study

The thermodynamic functions of Malachite Green (MG) dye adsorption on the prepared nanofiber membranes were calculated to understand the nature of the adsorption process, as shown in Table 6. The Gibbs free energy ( $\Delta G^\circ$ ) was calculated from Equation 6 [42]. Using the van't Hoff Equation 7, the enthalpy of adsorption ( $\Delta H^\circ$ ) was calculated from the slope of the linear equation when plotting  $\text{Ln}k$  versus the reciprocal of temperature  $1/T$  as in Figure 12 [43]. The value of the change in entropy ( $\Delta S^\circ$ ) was found through the Gibbs-Helmholtz

Equation 8 [44].

$$\Delta G^\circ = -RT \text{Ln}K \quad (\text{Eq.6})$$

$$\text{Ln}k = \frac{-\Delta H^\circ}{RT} + \text{constant} \quad (\text{Eq.7})$$

$$\Delta G^\circ = \Delta H^\circ - T\Delta S^\circ \quad (\text{Eq.8})$$

$k$ : thermodynamic equilibrium constant;  $R$ : the general gas constant ( $8.314 \text{ J mol}^{-1} \text{ K}^{-1}$ );  $T$ : absolute temperature ( $K$ ).

Table 6 shows that the values of  $\Delta G^\circ$  are negative for all the studied temperatures, which means that the adsorption process of Malachite Green dye on the prepared nanofiber membranes is spontaneous. This means that the dye molecules adhere to the nanofibers automatically and quickly over a wide range of temperatures. It is also noted that  $\Delta G^\circ$  becomes more negative at temperatures from 298 to 318 °K, which means that the adsorption process becomes more spontaneous with increasing temperature [45]. The positive  $\Delta H^\circ$  value ( $+20563.847 \text{ J mol}^{-1}$ ) indicates that the process is endothermic, i.e., adsorption requires energy (heat) to occur. This is consistent with the fact that the spontaneity of adsorption (negative  $\Delta G^\circ$ ) increases with increasing temperature, which means that providing heat enhances the adsorption process. This was confirmed by studying the effect of temperature and calculating the adsorption ratio, as the adsorption capacity increased with increasing temperature until it reached 92.946% at 318 °K [46]. Also, the positive value of  $\Delta H^\circ$  indicates that the adsorption process includes the diffusion of dye molecules within the internal pores of the nanofiber surface, reaching the internal active sites, and that this diffusion increases with increasing temperature [47,48]. In general, positive values of  $\Delta S^\circ$  mean that the process increases the randomness (Entropy) of the system. In other words, after adsorption, there is a more random distribution of dye molecules on the

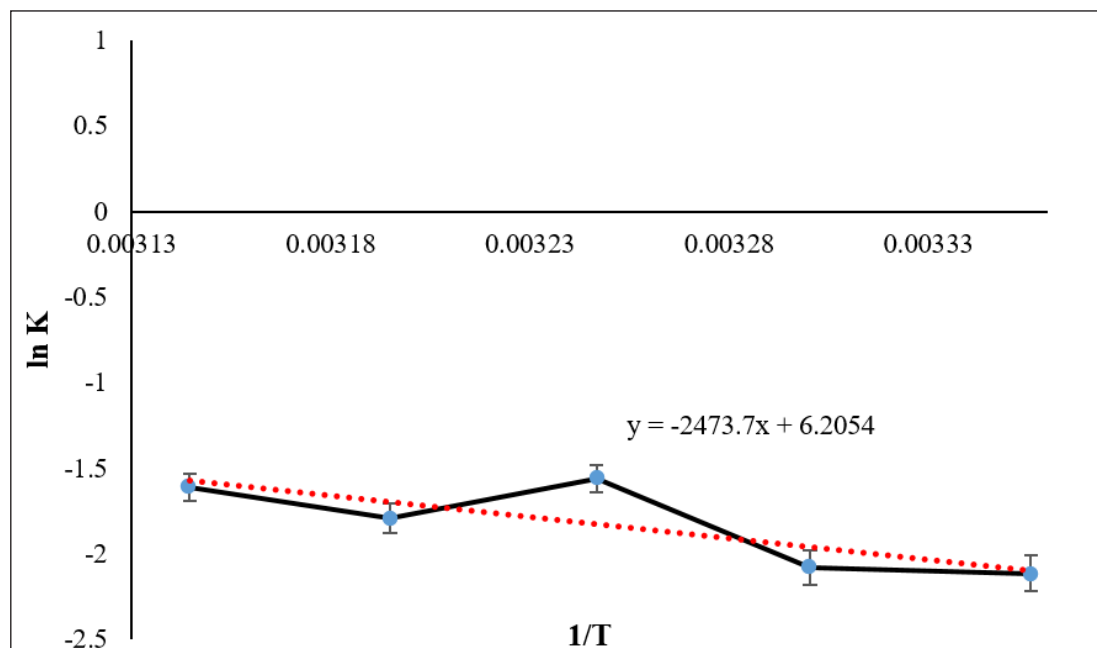


**Fig. 12.** Plot of  $1/T$  vs  $\ln K$  for adsorption of MG dye on the prepared nanofiber membranes

**Table 6.** Thermodynamic functions for adsorption of MG dye on the prepared nanofiber membranes

Temperature (K)	$\Delta G^\circ$ ( $J\ mole^{-1}$ )	$\Delta H^\circ$ ( $J\ mole^{-1}$ )	$\Delta S^\circ$ ( $J\ mole^{-1}$ )
298	-5238.91		+86.58642
303	-5238.41		+85.15596
308	-3989.96	+20563.847	+79.72015
313	-4662.66		+80.59588
318	-4255.12		+78.04705

surfaces of the nanofibers compared to the previous case, and this is due to the diffusion process accompanying the adsorption process [49,50].

#### 4. Conclusion

The nanofiber membranes were prepared using the electrospinning technique from suitable resin and morphologically characterized. The adsorption of Malachite Green (MG) dye from aqueous solutions on these nanofibers was studied, which included the

factors affecting the adsorption process, adsorption isotherms, and adsorption thermodynamics. The results showed that the prepared nanofiber membranes are very effective adsorbents due to their unique chemical and physical properties. MG dye was removed with an adsorption efficiency of up to 92.946% at 318 °K. The adsorption process is spontaneous and endothermic, which makes it a very effective and economical adsorbent that can be used as a filter for wastewater treatment.

## 5. Acknowledgements

We thank and appreciate the staff and management of the Physical Chemistry Laboratory, Ibn Al-Haitham College of Pure Sciences, University of Baghdad.

## 6. References

- [1] A.J. Ibrahim, ZnO nanostructure synthesis for the photocatalytic degradation of azo dye methyl orange from aqueous solutions utilizing activated carbon, *Anal. Meth. Environ. Chem. J.*, 5 (2022) 5-19. <https://doi.org/10.24200/amecj.v5.i04.200>
- [2] J.A. Naser, T.A. Himdan, A.J. Ibraheim, Adsorption kinetic of malachite green dye from aqueous solutions by electrospun nanofiber Mat, *Orient. J. Chem.*, 33 (2017) 3121-3129. <http://dx.doi.org/10.13005/ojc/330654>
- [3] G. A. Ismail, H. Sakai, Review on effect of different type of dyes on advanced oxidation processes (AOPs) for textile color removal, *Chemosphere*, 291 (2022) 132906. <https://doi.org/10.1016/j.chemosphere.2021.132906>
- [4] A. Debroy, M. Yadav, R. Dhawan, S. Dey, N. George, DNA dyes: toxicity, remediation strategies and alternatives, *Folia Microbiol.*, 67 (2022) 555-571. <https://doi.org/10.1007/s12223-022-00963-8>
- [5] R. H. Althomali, M. K. Abbood, F. M. Altalbawy, E. A. M. Saleh, S. S. Abdullaev, A. J. Ibrahim, S. A. Ansari, R. M. Romero-Parra, A novel nanomagnetic palladium (II) complex of bisimidazolium-based heterocyclic carbene; An efficient heterogeneous catalyst for A3 coupling reactions, *J. Mol. Struct.*, 1290 (2023) 135911. <https://doi.org/10.1016/j.molstruc.2023.135911>
- [6] B. T. Sayed, M.M. Al-Sakhnini, A.A. Alzubaidi, A. H. Alawadi, A. J. Ibrahim, S. Askar, Assessment of nano-imprinting process in CuZr amorphous films through combination of machine learning and molecular dynamics, *J. Electron. Mater.*, 52 (2023) 6943-6958. <https://doi.org/10.1007/s11664-023-10630-4>
- [7] L. Li, W. Guo, S. Zhang, R. Guo, L. Zhang, Electrospun nanofiber membrane: an efficient and environmentally friendly material for the removal of metals and dyes, *Molecules*, 28 (2023) 3288. <https://doi.org/10.3390%2Fmolecules28083288>
- [8] D. Pathak, A. Sharma, D. P. Sharma, V. Kumar, A review on electrospun nanofibers for photocatalysis: Upcoming technology for energy and environmental remediation applications, *Appl. Surf. Sci. Adv.*, 18 (2023) 100471. <https://doi.org/10.1016/j.apsadv.2023.100471>
- [9] A. j. Ibrahim, A.H. AL-Saeed, Evaluation of oxidative status, potassium, magnesium, and lipid profile in serum of patients with  $\beta$ -thalassemia major, Thi-Qar, Iraq, *Maaen J. Med. Sci.*, 2 (2023) 108-115. <https://doi.org/10.55810/2789-9128.1029>
- [10] A.j. Ibrahim, A.H. AL-Saeed, Evaluation of some heart enzymes and Iron levels in  $\beta$ -thalassemia patients in Thi-Qar city, Iraq, *Baghdad Sci. J.*, 21 (2024) 2007-2016. <https://doi.org/10.21123/bsj.2023.8352>
- [11] A. J. Ibrahim, Evaluation of oxidative stress in postmenopausal Iraqi women, *Al-Kuno. Sci. J.*, 8 (2024) 95-108. <http://doi.org/10.36582/j.alkuno.2024.08.05>
- [12] S. I. S. Al-Hawary, E. A. M.Saleh, N. A. Mamajanov, N. S. Gilmanova, H. O. Alsaab, A. Alghamdi, S.A. Ansari, A.H.R. Alawady, A. H. Alsaalamy, A. J. Ibrahim, Breast cancer vaccines; A comprehensive and updated review, *Pathol. Res. Pract.*, 249 (2023) 154735. <https://doi.org/10.1016/j.prp.2023.154735>
- [13] S. I. S. Al-Hawary, N. A. Tayyib, P. Ramaiah, R. M. R. Parra, A. J. Ibrahim, Y. F. Mustafa, B. M. Hussien, S. A. Alsulami, K. J. Baljon, I. Nomani, Functions of LncRNAs, exosomes derived MSCs and immune regulatory molecules in preeclampsia disease, *Pathol. Res. Pract.*, 250 (2023) 154795. <https://doi.org/10.1016/j.prp.2023.154795>
- [14] N. Amirinejad, A. Shekarchizadeh, M. Mousavi, M. A. Behzadi, M. Hassanshahian, S. A. Ataie, A. Hjazi, A. J. Ibrahim, Structural

- characterization of biosurfactant produced by marine bacterium *Pseudomonas fragi* strain F1 (isolated from Persian Gulf) and evaluation of antimicrobial and antibiofilm activity, *Res. Square*, 1 (2023). <https://doi.org/10.21203/rs.3.rs-3062097/v1>
- [15] A. j. Ibrahim, H.A.W. Dwesh, R.A. Shahid, Evaluation of serum leptin levels in hypertensive men in Thi Qar City-Iraq (a comparative study), *J. Pop. Therapeut. Clin. Pharmacol.*, 30 (2023) 54-62. <https://doi.org/10.47750/jptcp.2023.30.03.007>
- [16] R. Margiana, R. Gupta, W. M. Al-Jewari, A. Hjazi, H.O. Alsaab, Y.F. Mustafa, R. Singh, R. Thaibt, S. Alkhayyat, A. J. Ibrahim, Evaluation of telomere length, reactive oxygen species, and apoptosis in spermatozoa of patients with oligospermia, *Cell Biochem. Funct.*, 42 (2024) e3935. <https://doi.org/10.1002/cbf.3935>
- [17] A. J. Ibrahim, the Determination and evaluation of trace elements in the blood of radiography workers using graphite furnace atomic absorption spectrometry, *Anal. Meth. Environ. Chem. J.*, 7 (2024) 76-85. <https://doi.org/10.24200/amecj.v6.i04.321>
- [18] P. Nickl, J. Radnik, W. Azab, I. S. Donskyi, Surface characterization of covalently functionalized carbon-based nanomaterials using comprehensive XP and NEXAFS spectroscopies, *Appl. Surf. Sci.*, 613 (2023) 155953. <https://doi.org/10.1016/j.apsusc.2022.155953>
- [19] A.J. Ibrahim, Ultraviolet-activated sodium perborate process (UV/SPB) for removing humic acid from water, *Anal. Meth. Environ. Chem. J.*, 5 (2022) 5-18. <https://doi.org/10.24200/amecj.v5.i03.191>
- [20] B. Sarkodie, J. Amesimeku, C. Frimpong, E. K. Howard, Q. Feng, Z. Xu, Photocatalytic degradation of dyes by novel electrospun nanofibers: A review, *Chemosphere*, 313 (2023) 137654. <https://doi.org/10.1016/j.chemosphere.2022.137654>
- [21] A. J. Ibrahim, Adsorption behavior of Crystal Violet dye in aqueous solution using  $\text{Co}^{+2}$  hectorite composite as adsorbent surface, *Anal. Meth. Environ. Chem. J.*, 6 (2023) 5-16. <https://doi.org/10.24200/amecj.v6.i01.219>
- [22] A. J. Ibrahim, H. A. W. Dwesh, A. R. Al-Sawad, Adsorption of methylene blue dye onto bentonite clay: Characterization, adsorption isotherms, and thermodynamics study by using UV-Vis technique, *Anal. Meth. Environ. Chem. J.*, 6 (2023) 5-18. <https://doi.org/10.24200/amecj.v6.i03.243>
- [23] A. K. Dhar, H. A. Himu, M. Bhattacharjee, M. G. Mostufa, F. Parvin, Insights on applications of bentonite clays for the removal of dyes and heavy metals from wastewater: a review, *Environ. Sci. Pollut. Res.*, 30 (2023) 5440-5474. <https://doi.org/10.1007/s11356-022-24277-x>
- [24] H. S. Karapinar, F. Kilicel, F. Ozel, A. Sarilmaz, Fast and effective removal of Pb (II), Cu (II) and Ni (II) ions from aqueous solutions with  $\text{TiO}_2$  nanofibers: Synthesis, adsorption-desorption process and kinetic studies, *Int. J. Environ. Anal. Chem.*, 103 (2023) 4731-4751. <https://doi.org/10.1080/03067319.2021.1931162>
- [25] J. Debord, K. H. Chu, M. Harel, S. Salvestrini, J. C. Bollinger, Yesterday, today, and tomorrow. Evolution of a sleeping beauty: The Freundlich isotherm, *Langmuir*, 39 (2023) 3062-3071. <https://doi.org/10.1021/acs.langmuir.2c03105>
- [26] S. V. Langwald, A. Ehrmann, L. Sabantina, Measuring physical properties of electrospun nanofiber mats for different biomedical applications, *Membranes*, 13 (2023) 488. <https://doi.org/10.3390/membranes13050488>
- [27] J. Arévalo-Fester, A. Briceño, Insights into selective removal by dye adsorption on hydrophobic vs multivalent hydrophilic functionalized MWCNTs, *ACS Omega*, 8 (2023) 11233-11250. <https://doi.org/10.1021/acsomega.2c08203>
- [28] A. Naderahmadian, B. Eftekhari-Sis, H. Jafari, M. Zirak, M. Padervand, G. Mahmoudi, M. Samadi. Cellulose nanofibers decorated with  $\text{SiO}_2$  nanoparticles: Green adsorbents for removal of cationic and anionic dyes; kinetics,

- isotherms, and thermodynamic studies, *Int. J. Biol. Macromol.*, 247 (2023) 125753. <https://doi.org/10.1016/j.ijbiomac.2023.125753>
- [29] B. M. Thamer, F. A. Al-aizari, Highly efficient and reusable polymeric nanofibers for cationic dye removal: isotherm, kinetics and thermodynamic study, *New J. Chem.*, 48 (2024) 1414-1423. <https://doi.org/10.1039/D3NJ04757A>
- [30] S. T. Al-Asadi, F. F. Al-Qaim, H. F. S. Al-Saedi, I. F. Deyab, H. Kamyab, S. Chelliapan, Adsorption of methylene blue dye from aqueous solution using low-cost adsorbent: kinetic, isotherm adsorption, and thermodynamic studies, *Environ. Monit. Assess.*, 195 (2023) 676. <https://doi.org/10.1007/s10661-023-11334-2>
- [31] A. Yar, Ş. Parlayici, Carbon nanotubes/polyacrylonitrile composite nanofiber mats for highly efficient dye adsorption, *Colloids Surf. A: Physicochem. Eng. Asp.*, 651 (2022) 129703. <https://doi.org/10.1016/j.colsurfa.2022.129703>
- [32] H. N. Tran, Improper estimation of thermodynamic parameters in adsorption studies with distribution coefficient  $KD$  ( $q_e/C_e$ ) or Freundlich constant ( $KF$ ): Considerations from the derivation of dimensionless thermodynamic equilibrium constant and suggestions, *Adsorpt. Sci. Technol.*, 2022 (2022) 5553212. <https://doi.org/10.1155/2022/5553212>
- [33] E. Rápó, S. Tonk, Factors affecting synthetic dye adsorption; desorption studies: a review of results from the last five years (2017–2021), *Molecules*, 26 (2021) 5419. <https://doi.org/10.3390/molecules26175419>
- [34] A. Faghihi-Zarandi, J. Rakhshshah, B. Bahrami Yarahmadi, A rapid removal of xylene vapor from environmental air based on bismuth oxide coupled to heterogeneous graphene/graphene oxide by UV photo-catalectic degradation-adsorption procedure, *J. Environ. Chem. Eng.*, 8 (2020) 104193. <https://doi.org/10.1016/j.jece.2020.104193>
- [35] S. Teimoori, A. H. Hassani, M. Panahi, N. Mansouri, An immobilization of aminopropyl trimethoxysilane-phenanthrene carbaldehyde on graphene oxide for toluene extraction and separation in water samples, *Chemosphere*, 316 (2023) 137800. <https://doi.org/10.1016/j.chemosphere.2023.137800>
- [36] S. Teimoori, A. H. Hassani, M. Panahi, N. Mansouri, Rapid extraction of BTEX in water and milk samples based on functionalized MWCNTs by dispersive homogenized-micro-solid phase extraction, *Food Chem.*, 421 (2023) 136229. <https://doi.org/10.1016/j.foodchem.2023.136229>
- [37] S. Teimoori, A. H. Hassani, New extraction of toluene from water samples based on nano-carbon structure before determination by gas chromatography, *Int. J. Environ. Sci. Technol.*, 20 (2023) 6589–6608. <https://doi.org/10.1007/s13762-023-04906-9>
- [38] M. Mohammadi Asl, N. Mansouri, S. A. R. Haji Seyed Mirzahosseini, F. Atabi, Simultaneity comparative evaluation of toluene removal from the air by adsorption and UV semi-degradation-based adsorption procedure, *Int. J. Environ. Sci. Technol.*, 21 (2024) 6677-6694. <https://doi.org/10.1007/s13762-024-05503-0>
- [39] M. M. Asl, F. Atabi, Functionalized graphene oxide with bismuth and titanium oxide nanoparticles for efficiently removing formaldehyde from the air by photocatalytic degradation-adsorption process, *J. Anal. Test.*, 7 (2023) 444-458. <https://doi.org/10.1007/s41664-023-00272-0>
- [40] J. Rakhshshah, N. Esmaeil, A rapid extraction of toxic styrene from water and wastewater samples based on hydroxyethyl methylimidazolium tetrafluoroborate immobilized on MWCNTs by ultra-assisted dispersive cyclic conjugation-micro-solid phase extraction, *Microchem. J.*, 170 (2021) 106759. <https://doi.org/10.1016/j.microc.2021.106759>
- [41] M. Arjomandi, H. Shirkhanloo, A review: analytical methods for heavy metals determination in environment and human samples, *Anal. Methods Environ. Chem. J.*, 2 (2019) 97-126. <https://doi.org/10.24200/>

- amecj.v2.i03.73
- [42] M. Sheikhi, H. Rezaei, Efficient adsorption of nickel and chromium (VI) from aqueous solutions using lignocellulose nanofibers: Kinetics, isotherms, and thermodynamic studies, *Water Pract. Technol.*, 18 (2023) 1022-1038. <https://doi.org/10.2166/wpt.2023.054>
- [43] S. Sharafinia, A. Farrokhnia, E. G. Lemraski, Optimized safranin adsorption onto poly (vinylidene fluoride)-based nanofiber via response surface methodology, *Mater. Chem. Phys.*, 276 (2022) 125407. <https://doi.org/10.1016/j.matchemphys.2021.125407>
- [44] A. V. Dolganov, V. D. Revin, S. G. Kostyukov, V. V. Revin, G. Yang, Kinetic and thermodynamic characteristics of fluoride ions adsorption from solution onto the aluminum oxide nanolayer of a bacterial cellulose-based composite material, *Polymers*, 13 (2021) 3421. <https://doi.org/10.3390/polym13193421>
- [45] X. Zheng, T. Bian, Y. Zhang, Y. Zhang, Z. Li, Construction of ion-imprinted nanofiber chitosan films using low-temperature thermal phase separation for selective and efficient adsorption of Gd (III), *Cellulose*, 27 (2020) 455-467. <https://doi.org/10.1007/s10570-019-02804-3>
- [46] M. Gouda, A. Aljaafari, Removal of heavy metal ions from wastewater using hydroxyethyl methacrylate-modified cellulose nanofibers: kinetic, equilibrium, and thermodynamic analysis, *Int. J. Environ. Res. Public Health*, 18 (2021) 6581. <https://doi.org/10.3390/ijerph18126581>
- [47] A. E. Ofomaja, E. B. Naidoo, A. Pholosi, Intraparticle diffusion of Cr (VI) through biomass and magnetite coated biomass: A comparative kinetic and diffusion study, *South Afr. J. Chem. Eng.*, 32 (2020) 39-55. <https://hdl.handle.net/10520/EJC-1d7a4c6819>
- [48] F. Golbabaeei, Z. Sadeghi, A. Vahid, A. Rashidi, On-line micro column preconcentration system based on amino bimodal mesoporous silica nanoparticles as a novel adsorbent for removal and speciation of chromium (III, VI) in environmental samples, *J. Environ. Health Sci. Eng.*, 13 (2015) 1-12. <https://doi.org/10.1186/s40201-015-0205-z>
- [49] M. K. Abbasabadi, Speciation of cadmium in human blood samples based on Fe<sub>3</sub>O<sub>4</sub>-supported naphthalene-1-thiol- functionalized graphene oxide nanocomposite by ultrasound-assisted dispersive magnetic micro solid phase extraction, *J. Pharm. Biomed. Anal.*, 189 (2020)113455. <https://doi.org/10.1016/j.jpba.2020.113455>
- [50] K. S. Obayomi, J. O. Bello, M. D. Yahya, E. Chukwunedum, J. B. Adeoye, Statistical analyses on effective removal of cadmium and hexavalent chromium ions by multiwall carbon nanotubes (MWCNTs), *Heliyon*, 6 (2020) e04047. <https://doi.org/10.1016/j.heliyon.2020.e04174>